COMPDYN 2015
5th ECCOMAS Thematic Conference on
Computational Methods in Structural Dynamics and Earthquake Engineering
M. Papadrakakis, V. Papadopoulos, V. Plevris (eds.)
Crete Island, Greece, 25–27 May 2015

THE IMPACT OF VERTICAL HUMAN-STRUCTURE INTERACTION FOR FOOTBRIDGES

Katrien Van Nimmen[1,2], Kristof Maes[1], Geert Lombaert[1], Guido De Roeck[1] and Peter Van den Broeck[1,2]

[1] KU Leuven, Department of Civil Engineering, Structural Mechanics
B-3001 Leuven, Belgium
e-mail: katrien.vannimmen@kuleuven.be

[2] KU Leuven, Department of Civil Engineering, Technology Cluster Construction
B-9000 Ghent, Belgium
e-mail: peter.vandenbroeck@kuleuven.be

Keywords: human-structure interaction, footbridge, human-induced vibrations, vibration serviceability, full-scale testing.

Abstract. *To allow for a more accurate description of crowd-induced loading, the present study aims to provide the necessary insights into vertical human-structure interaction (HSI) phenomena, to date ignored in current load models. A parametric study is performed to investigate the effects of the mechanical interaction between pedestrians, represented by simple lumped parameter models, and the supporting footbridge. The most significant HSI-effect for the low-frequency modes of a footbridge, is in the effective damping ratio of the coupled system which is much higher than the inherent structural damping. The effective damping ratio increases monotonically with the pedestrian density but is highly dependent on the natural frequency of the footbridge. In order to verify the findings, a comprehensive full-scale experimental study is performed on two footbridges. It is shown that the crowd-structure model is able to reproduce the experimentally identified dynamic characteristics of the coupled system.*

1 INTRODUCTION

The relatively small service loads allows for very slender and lightweight footbridge designs. Characterised by a low stiffness to mass ratio, footbridges often have one or more natural frequencies below 6 Hz. Given the force spectrum of pedestrian excitation which is dominated by contributions around the fundamental ($1.25 - 2.50$ Hz) and the second ($2.50 - 5.00$ Hz) harmonic of the walking load, the vibration serviceability of footbridges is mostly governed by (near-)resonant loading [1, 2].

In the prediction of crowd-induced vibrations, persons crossing a footbridge are often simplified to (moving) forces [3]. However, this approach does not consider that people are mechanical systems which interact with the structure that is supporting them [4]. In some cases, the modal characteristics of the coupled crowd-structure system significantly differ from those of the empty footbridge [5, 6, 7]. The degree to which the dynamic behaviour is modified is expected to increase with an increasing crowd to structural mass ratio. Hence, these effects are expected to be non-negligible for lightweight footbridges [8, 9].

To characterise HSI-effects for slender footbridges, the low-frequency behaviour of the human body ($<$ 10 Hz) is of interest in this paper. As the human dynamics in the vertical direction largely depends on the body posture [10], a distinction is made between *active* and *passive* postures as assumed by active (e.g. walking, jogging, ...) and passive (e.g. standing still) persons, respectively. Passive persons are most likely to assume a standing posture characterised by legs being straight. On the other hand, the posture of an active individual is changing continuously during the gait cycle and it involves either one or two legs slightly bent.

In the present work, the effects of the mechanical interaction between pedestrians and the supporting footbridge are investigated by means of a parametric study. The latter considers a realistic crowd model, composed of active and passive individuals and subject to inter-person variability.

The outline of this paper is as follows. First, the low-frequency dynamic properties of the footbridge and the human body are discussed and the coupled human-structure model is presented. Second, the implications for the practical design of footbridges are evaluated based on a realistic crowd model representative of the inter-person variability. Finally, the predicted dynamic behaviour of the coupled human-structure system is verified by means of field-tests on two footbridges.

2 FRAMEWORK

This section aims at providing a concise and structured overview of the relevant dynamic properties of footbridges and the human body with the prime purpose to determine realistic parameter ranges for the parametric study.

2.1 Dynamic behaviour of footbridges

The low-frequency dynamic behaviour of footbridges is characterised by the modal properties [1], i.e. the natural frequencies $f_{\mathrm{B}j}$, modal damping ratios $\xi_{\mathrm{B}j}$ and modal masses $m_{\mathrm{B}j}$, of the low-frequency vibration modes. During the last decade, numerous experimental studies of the dynamic behaviour of footbridges have been performed. The following paragraphs present a synopsis of the relevant modal properties reported in literature. The collected footbridge data are composed of 11 structures investigated by the authors and over 100 footbridges discussed in other reports and publications. The main sources of information used are the SYNPEX report [2], the French Sétra guideline [11], the JRC document for the design of lightweight footbridges

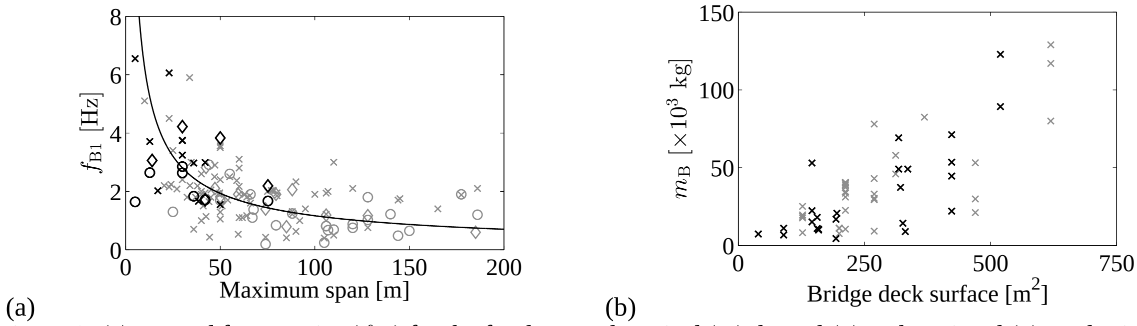

Figure 1: (a) Natural frequencies (f_{B1}) for the fundamental vertical ($\times$), lateral ($\circ$) and torsional ($\diamond$) modes in terms of the maximum span length of the footbridge, (b) modal mass (m_{B}) in terms of the total bridge deck surface: as reported in literature (grey), for the 11 cases investigated by the authors (black) and the relationship defined in [15] (line).

[12] and the reference lists of GERB [13] and MAURER-SÖHNE [14].

Figure 1-a presents the identified natural frequencies in relation to the maximum span length, including only the first (fundamental) lateral, vertical and/or torsional mode. As expected, the natural frequencies tend to decrease with increasing span length. However, even bridges with short spans can exhibit low natural frequencies (< 6 Hz) which is due to the distinct slender designs. The collected data qualitatively agree with the natural frequency to span relationship as proposed by Bachmann et al. [15] based on data for 67 footbridges with spans between 15 and 50 metres:

$$f_{\mathrm{B1}} = 33.6\, l^{-0.73} \tag{1}$$

where f_{B1} [Hz] denotes the fundamental natural frequency and l [m] the span of the footbridge (figure 1).

The second modal property of interest is the modal mass. When obtained via the unity-scaled mode shapes, the modal mass is a measure of the physical mass of the system that is engaged in a particular mode [16]. The modal masses reported in literature include both experimentally identified and numerically calculated values. Figure 1-b presents the reported modal masses in relation to the total bridge deck surface. As expected, the modal masses increase with increasing functional area.

The third relevant modal property is the modal damping ratio. Design guides for the vibration serviceability assessment of footbridges propose numerical values for the modal damping ratios based on experience obtained from similar construction types (table 1). Figure 2 presents the identified modal damping ratios for different construction types in relation to the corresponding natural frequency. This figure illustrates that the lowest modal damping ratios are retrieved for steel and composite bridges with minimum and mean values that agree with the provisional values reported by the guidelines (see table 1).

2.2 Dynamic behaviour of the human body

The low-frequency (0-10 Hz) dynamic behaviour of the human body in the vertical direction can be represented by a highly damped single degree of freedom (SDOF) system [21, 22, 23]. The mass $m_{\mathrm{H},k}$, being equal the total mass of the corresponding individual k, is divided into two lumped masses, i.e. a sprung mass $m_{\mathrm{H1},k}$ [21, 22, 24] and a rigid mass $m_{\mathrm{H0},k}$ at the support ($m_{\mathrm{H},k} = m_{\mathrm{H0},k} + m_{\mathrm{H1},k}$). The corresponding mechanical properties ($f_{\mathrm{H1},k}$ and $\xi_{\mathrm{H1},k}$) largely depend on the body posture [10]. On a footbridge, usually both active and passive persons are

Type	Bachmann [15] min	max	Sétra [11] min	mean	HiVoSS [17] min	mean	ISO 10137 [18]	EC 1 EC 5 [19, 20]
RC	0.8	2.0	0.8	1.3	0.8	1.3	0.8	1.5
PC	0.5	1.7	0.5	1.0	0.5	1.0	0.8	1.0
S	0.2	0.4	0.2	0.4	0.2	0.4	0.5	0.5
C	0.3	0.6	0.3	0.6	0.3	0.6	0.6	0.5
T	1.5	3.0	1.5	3.0	1.0	1.5	-	1.0-1.5
S-R	-	-	-	-	0.7	1.0	-	-

Table 1: Provisional modal damping ratios ξ_B [%] as suggested by the current codes of practice for different construction types: reinforced concrete (RC), prestressed concrete (PC), steel (S), composite (C), timber (T) and stress-ribbon (S-R).

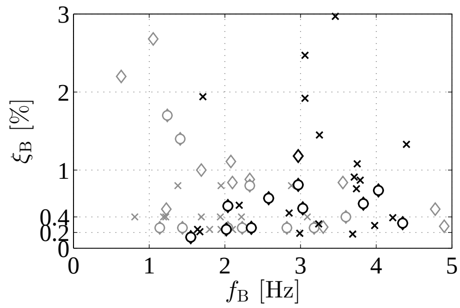

Figure 2: Identified modal damping ratios (ξ_B) for steel ($\times$), composite ($\circ$) and concrete ($\diamond$) footbridges in terms of the corresponding natural frequencies (f_B): as reported in literature (grey) and for the 11 cases investigated by the authors (black).

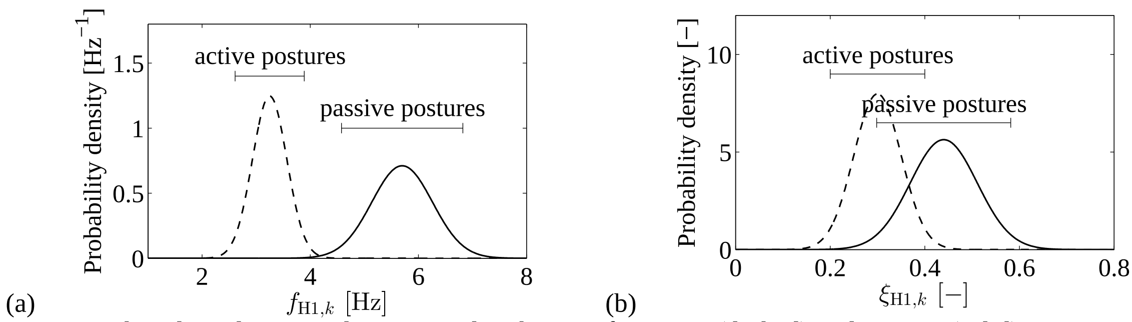

Figure 3: The adopted truncated Gaussian distributions for active (dashed) and passive (solid) postures: (a) the natural frequency $f_{H1,k}$ and (b) modal damping ratio $\xi_{H1,k}$.

present. Passive individuals most often assume a standing posture whereas the posture of active individuals is changing continuously during the walking cycle. In the following, active persons are represented by (stationary) human body models representative of a body posture with one or two legs, i.e. considered in this paper as an approximation of the postures assumed during the walking cycle.

The fundamental natural frequency of an active person is situated between 2.5 Hz and 4 Hz with a corresponding modal damping ratio between 20% and 40% [22, 25]. For passive persons, the natural frequency and damping ratio are generally situated between 5.0-6.5 Hz and 35%-50%, respectively [22, 26]. In both cases, the mass $m_{H1,k}$ is found between 85% and 99% of the total mass $m_{H,k}$ with the remaining mass $m_{H0,k}$ lumped at the support.

In the following, inter-subject variability is accounted for by assuming a Gaussian distribution of the natural frequency and modal damping ratio of the human body model. The mean values and coefficient of variation are based on the results reported by Matsumoto and Griffin

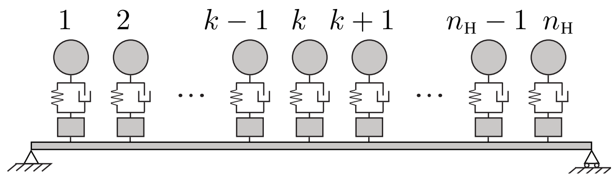

Figure 4: The coupled system composed of n_{H} persons and the supporting footbridge.

[22] and the results from an experimental study performed by the authors [25] (see figure 3):

$$\text{Passive persons:} \tag{2}$$
$$f_{\mathrm{H1},k} \sim \mathcal{N}(\mu_{f_{\mathrm{H1},k}}, \sigma_{f_{\mathrm{H1},k}}) = \mathcal{N}(5.7, 0.56) \qquad [\mathrm{Hz}] \tag{3}$$
$$\xi_{\mathrm{H1},k} \sim \mathcal{N}(\mu_{\xi_{\mathrm{H1},k}}, \sigma_{\xi_{\mathrm{H1},k}}) = \mathcal{N}(0.44, 0.07) \qquad [-] \tag{4}$$
$$\text{Active persons:} \tag{5}$$
$$f_{\mathrm{H1},k} \sim \mathcal{N}(\mu_{f_{\mathrm{H1},k}}, \sigma_{f_{\mathrm{H1},k}}) = \mathcal{N}(3.25, 0.32) \qquad [\mathrm{Hz}] \tag{6}$$
$$\xi_{\mathrm{H1},k} \sim \mathcal{N}(\mu_{\xi_{\mathrm{H1},k}}, \sigma_{\xi_{\mathrm{H1},k}}) = \mathcal{N}(0.30, 0.05) \qquad [-] \tag{7}$$

2.3 Coupled human-structure model

When a person is present on a footbridge, interaction occurs between his body and the structure. The two subsystems interact with each other through contact forces induced at the contact points between the person and the bridge deck, i.e. at the feet-bridge deck interface. In the following, both active and passive persons are modelled as stationary. The governing equations of motion can be written for two linear dynamic subsystems separately. In order to ensure coupling, compatibility and equilibrium conditions at the contact points need to be satisfied (analogous to the problem of vehicle-bridge interaction [27]). As the persons are assumed to be stationary, the coupled system is time-invariant. The reader is referred to [25] for a detailed description of the coupled system and corresponding system matrices.

3 PARAMETRIC STUDY

The HSI-effects are investigated for a realistic crowd model consisting of n_{H} individuals (n_{H} human body models), with a distribution of human body model parameters representative of inter-subject variability (see section 2.2). The observed quantities are evaluated using Monte Carlo simulations. Since the dynamic characteristics of the human body are quite different for active and passive body postures, the *activity ratio* is considered as an additional parameter here. A unit value of the activity ratio corresponds to the case where all the persons on the bridge are active. As it is expected that most people present on a footbridge are active, an activity ratio of 0.5 up to 1.0 is considered.

Natural frequencies between 0.5 Hz and 6.0 Hz are considered for the empty footbridge. In addition, the implications of HSI for practical design of footbridges are investigated assuming a range of: (i) the mass ratio ($0.02 \leq \mu_{\mathrm{HB}} \leq 0.50$ [-]) and (ii) the structural modal damping ratio ($\xi_{\mathrm{B}} = \{0.2, 0.5, 2.0\}$ [%]). To facilitate the practical interpretation, the results are expressed in terms of the natural frequency of the footbridge f_{B} [Hz].

First, the output quantities of interest are selected. Second, the Monte Carlo simulation of the crowd composition is discussed. Subsequently, the influence of the activity ratio and the structural modal damping ratio are investigated.

3.1 Output quantities of interest

The parametric study aims to determine when the interaction effects with the crowd are significant and whether or not they are beneficial. An interaction effect is here understood as beneficial if it reduces the maximum acceleration response of the footbridge. The vibration serviceability of footbridges is mostly governed by (near-)resonant loading [1]. For the empty footbridge, the maximum steady-state amplitude $\ddot{u}_{\mathrm{B,max}}$ to harmonic excitation is found as:

$$\ddot{u}_{\mathrm{B,max}} \sim \frac{1}{2\xi_{\mathrm{B}} m_{\mathrm{B}}} = |\mathrm{H}_{\mathrm{B}}(\omega_{\mathrm{B}})| \tag{8}$$

with $\mathrm{H}_{\mathrm{B}}(\omega)$ the frequency response function (FRF) of the footbridge and ω_{B} the natural frequency of the footbridge in rad/s. In this case, the natural frequency f_{B}, modal damping ratio ξ_{B} and modal mass m_{B} are the key parameters that determine the structural dynamic response.

Similarly, the FRF of the coupled system relating the harmonic input excitation to the acceleration response (in the following referred to as $\mathrm{H}_{\mathrm{HB}}(\omega)$), both taken at the footbridge DOF, is examined and its key parameters are identified. First, a reference case is defined for the coupled crowd-structure system. For this reference case, the HSI-effects are evaluated for a selection of frequency ($f_{\mathrm{H1}}/f_{\mathrm{B}}$) and mass ($\mu_{\mathrm{HB}}$) ratios. The selected case corresponds to a footbridge with a modal damping ratio of $\xi_{\mathrm{B}} = 0.5\%$, occupied by a crowd that is represented by the human body model with modal damping ratio $\xi_{\mathrm{H1}} = 40\%$ and mass ratio $\mu_{\mathrm{H1}} = 0.95$.

Figure 5-a presents the FRF of the coupled system $\mathrm{H}_{\mathrm{HB}}(\omega)$ for a fixed mass ratio ($\mu_{\mathrm{HB}} = 0.3$) and for ten different frequency ratios $f_{\mathrm{H1}}/f_{\mathrm{B}}$, uniformly spaced between 0.2 and 2. This figure illustrates that the FRF $\mathrm{H}_{\mathrm{HB}}(\omega)$, relating the harmonic input excitation to the acceleration response of the footbridge, is characterised by a single peak. Furthermore, figure 5-a shows that the peak value of $\mathrm{H}_{\mathrm{HB}}(\omega)$ highly depends on the frequency ratio $f_{\mathrm{H1}}/f_{\mathrm{B}}$, and, is at its lowest for frequency ratios $f_{\mathrm{H1}}/f_{\mathrm{B}}$ slightly lower than unity.

Figures 5-b and 5-c compare the FRF of the empty footbridge with the FRF of the coupled system for a mass ratio μ_{HB} of 0.1 and 0.4, respectively. Both figures present the FRF $\mathrm{H}_{\mathrm{HB}}(\omega)$ for five different frequency ratios $f_{\mathrm{H1}}/f_{\mathrm{B}} = \{0.4, 0.6, 0.8, 1.0, 1.2\}$. The peak value of the FRF of the coupled system is in all cases lower than the one of the empty footbridge. Comparing figure 5-b with figure 5-c shows that the interaction effects, i.e. the change of the peak value and corresponding frequency (abscissa), increase with the mass ratio, as expected. Furthermore, the frequency at which the corresponding peak value of $\mathrm{H}_{\mathrm{HB}}(\omega)$ is reached, also depends on the frequency ratio $f_{\mathrm{H1}}/f_{\mathrm{B}}$. For frequency ratios lower and higher than unity, this frequency is found above and below the natural frequency of the empty footbridge, respectively.

The peak value of the FRF $\mathrm{H}_{\mathrm{HB}}(\omega)$ determines the maximum amplitude of the steady-state acceleration response of the footbridge $\ddot{u}_{\mathrm{HB,max}}$ when subjected to harmonic excitation:

$$\begin{aligned} &\ddot{u}_{\mathrm{HB,max}} \sim |\mathrm{H}_{\mathrm{HB}}(\omega_{\mathrm{HB}})|\,, \\ &\text{with} \quad \omega_{\mathrm{HB}} = \underset{\omega}{\operatorname{argmax}}\,|\mathrm{H}_{\mathrm{HB}}(\omega)| \end{aligned} \tag{9}$$

The effective natural frequency of the coupled system f_{eff} [Hz] is now defined as:

$$f_{\mathrm{eff}} = \frac{\omega_{\mathrm{HB}}}{2\pi} \tag{10}$$

Accordingly, the effective damping ratio ξ_{eff} [-] is defined as a measure for the change in maxi-

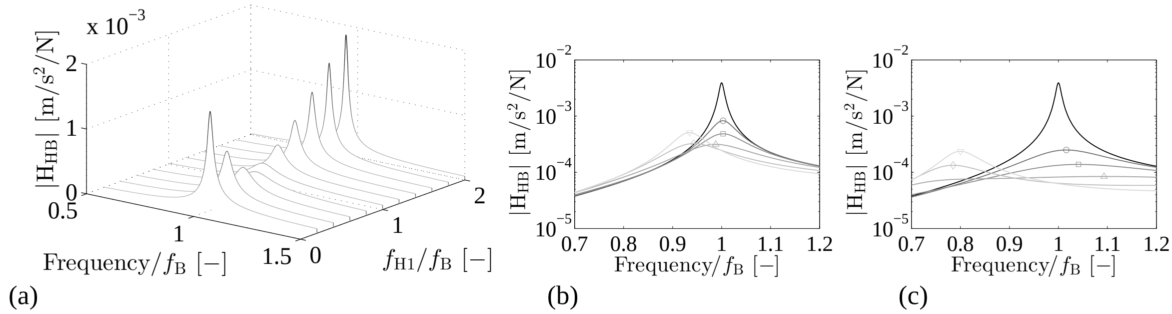

Figure 5: The FRF $\mathrm{H}_{\mathrm{HB}}(\omega)$ for a footbridge with $\xi_{\mathrm{B}} = 0.5\%$ coupled to the human body model with $\mu_{\mathrm{H1}} = 0.95$, $\xi_{\mathrm{H1}} = 40\%$ for a mass ratio of (a) $\mu_{\mathrm{HB}} = 0.3$, (b) $\mu_{\mathrm{HB}} = 0.1$ and (c) $\mu_{\mathrm{HB}} = 0.4$ for frequency ratio $f_{\mathrm{H1}}/f_{\mathrm{B}}$: 0.4 (○), 0.6 (□), 0.8 (△), 1.0 (◇) and 1.2 (▽), in terms of the frequency ratio ($f_{\mathrm{H1}}/f_{\mathrm{B}}$).

mum steady-state acceleration response in relation to that of the empty footbridge:

$$\begin{aligned} \ddot{u}_{\mathrm{HB,max}} &\sim \frac{1}{2\xi_{\mathrm{eff}} m_{\mathrm{B}}} \\ \Rightarrow \xi_{\mathrm{eff}} &= \frac{\ddot{u}_{\mathrm{B,max}}}{\ddot{u}_{\mathrm{HB,max}}}\,\xi_{\mathrm{B}} = \frac{|\mathrm{H}_{\mathrm{B}}(\omega_{\mathrm{B}})|}{|\mathrm{H}_{\mathrm{HB}}(\omega_{\mathrm{HB}})|}\,\xi_{\mathrm{B}} \end{aligned} \tag{11}$$

Finally, the reduction of the bridge acceleration due to human-structure interaction is described by the factor R_{HB} [-]:

$$R_{\mathrm{HB}} = \frac{\ddot{u}_{\mathrm{B,max}}}{\ddot{u}_{\mathrm{HB,max}}} = \frac{|\mathrm{H}_{\mathrm{B}}(\omega_{\mathrm{B}})|}{|\mathrm{H}_{\mathrm{HB}}(\omega_{\mathrm{HB}})|} \tag{12}$$

The interaction effect is beneficial when the reduction factor is larger than unity ($R_{\mathrm{HB}} > 1$) whereas it is disadvantageous when lower than unity ($R_{\mathrm{HB}} < 1$).

3.2 Monte Carlo Simulation of the crowd configuration

The crowd consists of an integer number of persons n_{H} (see figure 4 and section 2.3). Each individual is represented by a human body model with a mass $m_{\mathrm{H}} = 70$ kg. The number of persons n_{H} corresponding to a mass ratio μ_{HB} is calculated by assuming the previously introduced simply supported reference structure, with a total mass of 50 $\times 10^3$ kg (see section 3). This results in a number of 15 and 360 persons for the lower (0.02) and upper (0.50) limit of the considered mass ratios, respectively.

The human body model parameters (f_{H1} and ξ_{H1}) are sampled from the truncated distributions suggested in section 2.2. Since the influence of the mass ratio (μ_{H1}) was found to be insignificant, the corresponding parameter value is fixed at 0.95 [-]. The selected activity ratio defines the number of active and passive persons. The location of each individual is chosen randomly along the bridge deck assuming a uniform distribution (see figure 4).

For each crowd configuration, the normalised effective natural frequency $f_{\mathrm{eff}}/f_{\mathrm{B}}$ and effective damping ratio ξ_{eff} are calculated. In order to obtain a conservative (or *lower bound*) estimate of the interaction benefit, the 95%-percentile of the minimum effective damping ratio is evaluated [28]. For the normalised effective natural frequency, both the 5%-percentile and 95%-percentile value are equally relevant. For reasons of conciseness, only the percentile value corresponding to the largest modification in comparison to f_{B} is presented.

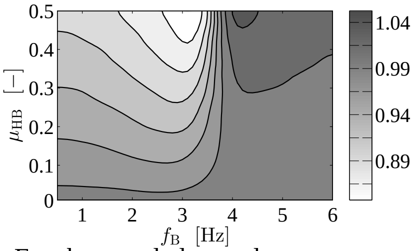

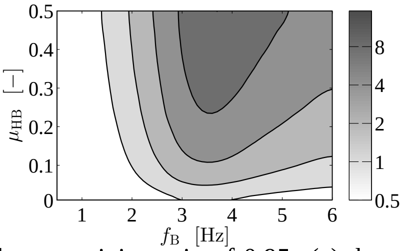

Figure 6: For the coupled crowd-structure system characterised by an activity ratio of 0.95: (a) the normalised effective natural frequency $f_{\mathrm{eff}}/f_{\mathrm{B}}$ and (b) effective damping ratio ξ_{eff} in terms of the natural frequency of the footbridge (f_{B}) and the considered mass ratios (μ_{HB}), for a footbridge with a modal damping ratio ξ_{B} of 0.5%.

3.3 HSI-effects for a reference case

As a starting point, the influence of HSI is discussed for a reference case. In this reference case, a structural modal damping ratio of $\xi_{\mathrm{B}} = 0.5\%$ is considered and the activity ratio of the crowd is set to 0.95. The HSI-effects are analysed for a natural frequency of the footbridge f_{B} between 0.5 Hz and 6.0 Hz and mass ratios μ_{HB} up to 0.5. Figure 6 presents the normalised effective natural frequency $f_{\mathrm{eff}}/f_{\mathrm{B}}$ and effective damping ratio ξ_{eff} in terms of the mass ratio and the natural frequency of the empty footbridge.

For low natural frequencies of the empty footbridge ($f_{\mathrm{B}} < 2.5$ Hz), the human body models are stiffer than the supporting structure and the HSI-effect is limited to that of an equivalent added mass: the natural frequencies reduce in relation to the considered mass ratio and the effective damping ratio approximately equals the modal damping ratio of the empty footbridge ($\xi_{\mathrm{eff}} \approx \xi_{\mathrm{B}}$).

For intermediate natural frequencies of the empty footbridge ($2.5 < f_{\mathrm{B}} < 4.5$ Hz), the effective natural frequency of the coupled system is slightly lower (for $f_{\mathrm{B}} < 3.25$ Hz) or higher (for $f_{\mathrm{B}} > 3.25$ Hz) than the natural frequency of the empty footbridge. More striking is the significant increase in the effective damping ratio. For low mass ratios, the effective damping ratio increases up to 1%-2% while for high mass ratios, the effective damping ratio easily exceeds 8%. This is due to the fact that the crowd is mainly composed of pedestrians with natural frequencies around 3.25 Hz for the considered high activity ratio. As a result, the frequency ratios are close to unity ($f_{\mathrm{H1}}/f_{\mathrm{B}} \approx 1$) and the corresponding HSI-effects are significant. In this case, the crowd behaves in a similar way as a tuned mass damper (TMD).

For high natural frequencies of the empty footbridge ($4.5 < f_{\mathrm{B}} < 6$ Hz), the effective damping ratio again increases with the mass ratio, but less strongly than for intermediate natural frequencies. For these frequency ratios, the crowd is more flexible than the footbridge and the two subsystems remain largely decoupled. For high mass ratios, the effective natural frequency is also slightly higher than the natural frequency of the empty footbridge while for low mass ratios, the HSI-effects are insignificant.

3.4 Influence of activity ratio

Figure 7 presents the normalised effective natural frequency ($f_{\mathrm{eff}}/f_{\mathrm{B}}$) and effective damping ratio (ξ_{eff}) in terms of the activity ratio and the natural frequency of the empty footbridge. The influence of the activity ratio on the HSI-effects is evaluated for four mass ratios μ_{HB}: 0.05, 0.10, 0.20 and 0.5. For the reference case, these mass ratios roughly correspond to pedestrian densities of 0.25, 0.5, 1.0 and 2.5 $\mathrm{persons/m^2}$, respectively. A fixed value is assumed for the modal damping ratio of the footbridge ($\xi_{\mathrm{B}} = 0.5\%$).

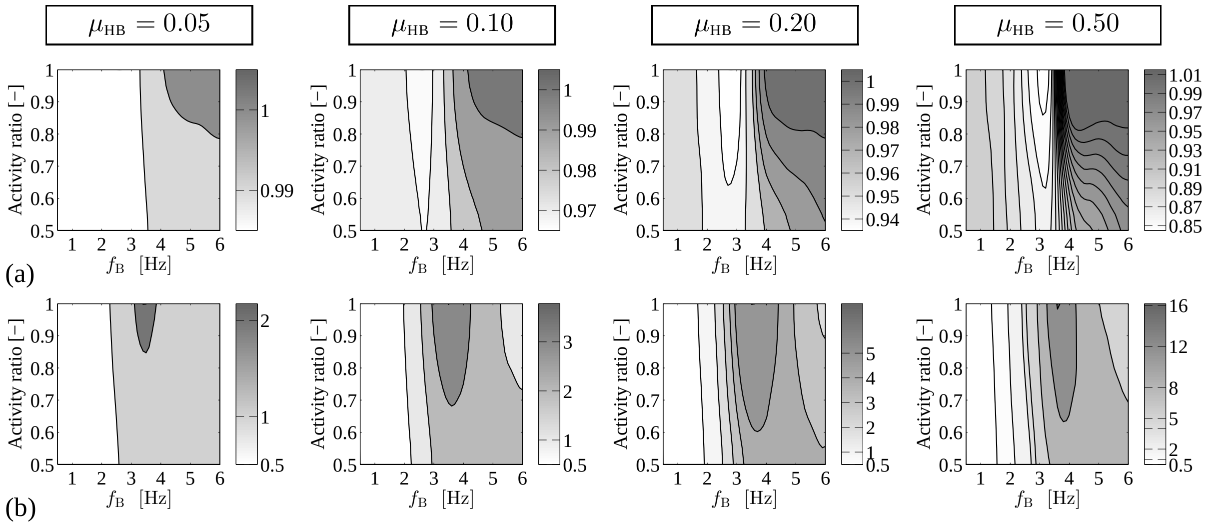

Figure 7: For the coupled crowd-structure system consisting of a footbridge with modal damping ratio $\xi_{\mathrm{B}} = 0.5\%$: (a) the normalised effective natural frequency $f_{\mathrm{eff}}/f_{\mathrm{B}}$ and (b) effective damping ratio ξ_{eff} for a mass ratio μ_{HB} of 0.05, 0.1, 0.2 and 0.5 in terms of the activity ratio and the natural frequency of the footbridge (f_{B}).

For low natural frequencies of the empty footbridge ($f_{\mathrm{B}} < 2.5$ Hz), the HSI-effects are independent of the activity ratio. As the crowd is composed of pedestrians with a natural frequency around 5.70 Hz or 3.25 Hz, the frequency ratios are, in both cases, relatively high ($f_{\mathrm{H1}}/f_{\mathrm{B}} > 1.5$). Hence, the pedestrians act as an equivalent added mass, regardless of their activity.

For intermediate natural frequencies of the empty footbridge ($2.5 < f_{\mathrm{B}} < 4.5$ Hz), the HSI-effects slightly decrease with a reducing activity ratio. A reduction of the activity ratio leads to a higher number of passive persons with corresponding frequency ratios ($f_{\mathrm{H1}}/f_{\mathrm{B}}$) that increase from approximately unity up to 1.75 and, therefore, leads to smaller HSI-effects.

Accordingly, *for high natural frequencies of the empty footbridge* ($f_{\mathrm{B}} > 4.5$ Hz), the HSI-effects are higher for lower activity ratios as this increases the number of individuals with a frequency ratio ($f_{\mathrm{H1}}/f_{\mathrm{B}}$) close to unity.

3.5 Influence of structural damping

Figure 7 presents the normalised effective natural frequency ($f_{\mathrm{eff}}/f_{\mathrm{B}}$) and effective damping ratio (ξ_{eff}) in terms of the mass ratio (μ_{HB}) and the natural frequency of the empty footbridge, for a fixed activity ratio of 0.95. The influence of the structural damping on the HSI-effects is investigated by considering three different modal damping ratios of the empty footbridge: $\xi_{\mathrm{B}} = \{0.2, 0.5, 2.0\}\,\%$.

Figure 7 shows that the effect of the structural damping ratio on the effective natural frequency of the coupled system, is insignificant.

For low natural frequencies of the empty footbridge ($f_{\mathrm{B}} < 2.5$ Hz), the effective damping ratio increases with the mass ratio and the natural frequency of the empty footbridge. For natural frequencies below 1.5 Hz, the effective damping ratio is close to the inherent structural damping. As the natural frequencies increase towards 2.5 Hz, the increase in effective damping ratio becomes significant. The lower the inherent structural damping, the stronger the increase in the effective damping ratio.

For intermediate natural frequencies of the empty footbridge ($2.5 < f_{\mathrm{B}} < 4.5$ Hz), the effec-

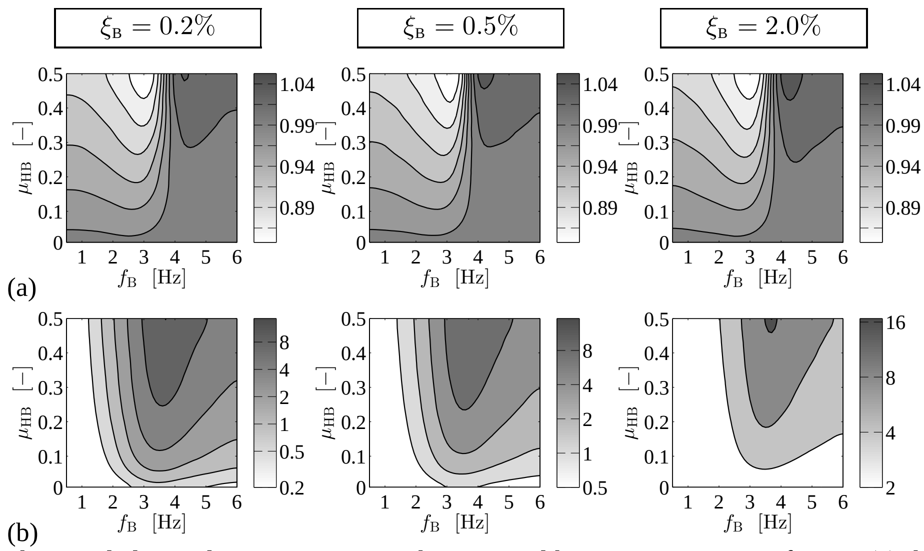

Figure 8: For the coupled crowd-structure system characterised by an activity ratio of 0.95: (a) the normalised effective natural frequency f_{eff}/f_B and (b) effective damping ratio ξ_{eff} (right) in terms of the natural frequency of the footbridge (f_B) and the considered mass ratios (μ_{HB}), for a footbridge with a modal damping ratio ξ_B of 0.2%, 0.5% and 2.0%.

tive damping ratio increases significantly with the mass ratio as the frequency ratios (f_{H1}/f_B) are close to unity. For low mass ratios, this HSI-effect is insignificant for structures with a relatively high inherent damping ($\xi_B \geq 2\%$). For very lowly-damped structures ($\xi_B \leq 0.5\%$) on the other hand, the increase in effective damping ratio is considerable, even for very low mass ratios. Note that for high mass ratios ($\mu_{HB} > 0.25$), the effective damping ratio reaches extremely high values ($\xi_{eff} > 8\%$), independently of the inherent structural damping.

For high natural frequencies of the empty footbridge ($4.5 < f_B < 6.0$ Hz), the effective damping ratio again increases significantly with the mass ratio, but less strong than for intermediate natural frequencies.

4 FULL-SCALE EXPERIMENTAL VERIFICATION

This section examines the effect of HSI based on in situ tests on two lightweight steel footbridges. By comparing the measured and predicted effective natural frequencies and modal damping ratios, it is verified if the coupled human-structure model allows reproducing the experimentally identified dynamic behaviour of the coupled system.

On the Eeklo footbridge, tests with both passive and active persons are performed. In addition, small-scale tests are performed on the Charleroi footbridge involving a limited number of pedestrians.

4.1 Eeklo footbridge

The experimental identification of the modal characteristics and the calibration of the numerical model of the Eeklo footbridge, was previously discussed in [29]. The two modes of interest in the present analysis are the fundamental lateral-torsional mode ($f_1 = 1.71$ Hz, $\xi_1 = 2.3\%$, $m_1 = 34 \times 10^3$ kg) and the first vertical bending mode ($f_2 = 2.99$ Hz, $\xi_2 = 0.2\%$, $m_2 = 22 \times 10^3$ kg). From the previous analyses, it is expected that the second mode will be strongly affected by the presence of persons on the bridge deck.

The structural response is registered during free vibration tests as well as trials involving

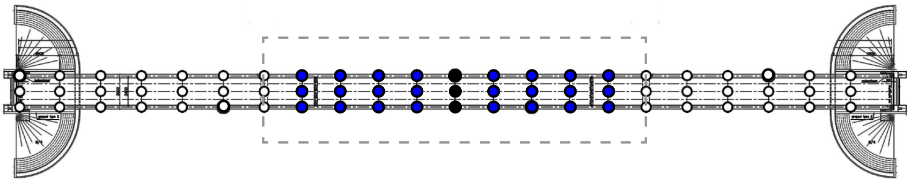

Figure 9: Top view of the Eeklo footbridge with walking area (box) and stationary subject locations (solid).

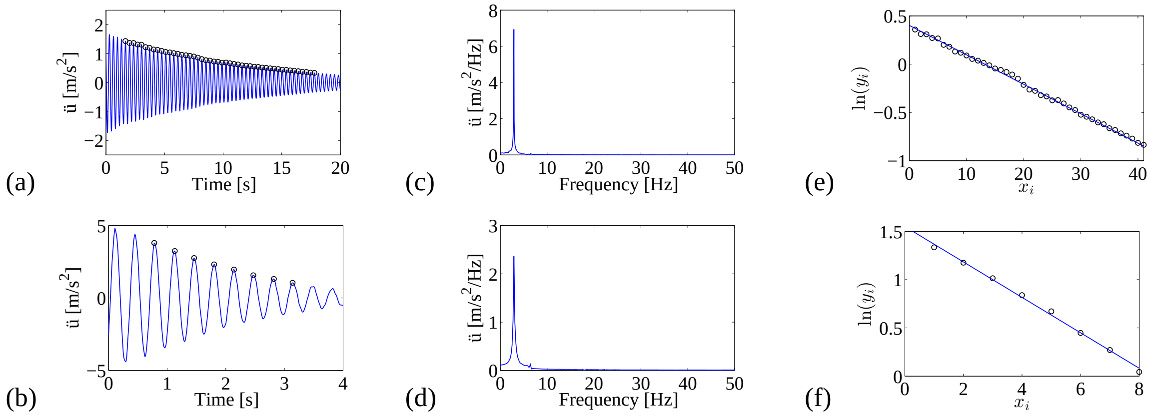

Figure 10: Measured vertical free vibration response of the footbridge at midspan with 15 human persons adopting the posture (a, c, e) with straight legs and (b, d, f) slightly bent legs: (a, b) time series with selected peak values, (c, d) corresponding amplitude spectrum and (e, f) natural logarithm and best-fit line of peak amplitudes (y_i) and abscissa (x_i).

ambient and random walking excitation. In order to obtain a free vibration dominated by the contribution of a single mode, the bridge is first brought into motion by rhythmical human activities (bobbing) tuned at the selected natural frequency using a metronome. Once the desired level of vibration is reached, the persons cease bobbing and get into the selected body posture, thereby initiating the free vibration phase. The natural frequency and damping ratio of the considered mode of the coupled system are subsequently identified from a free decay analysis. For the trials involving ambient and random walking excitation, the natural frequency and modal damping ratio of the first and the second mode of the coupled system are identified from an operational modal analysis.

Free decay analysis

The experiments include trials with a different number of persons on the bridge deck. Every individual is positioned at a point where a stringer crosses a cross girder. In the first setup, only three persons are positioned at midspan (figure 9). For each of the following setups, the number of persons is increased by six, three on the left and three on the right adjacent cross girder, respectively. For the setups involving the free vibration of the fundamental torsional mode, the persons on the central stringer are not included. In addition, the influence of the body posture on the dynamic behaviour of the coupled system is examined. The experiments therefore consider the human body in the normal standing posture with (1) straight legs and (2) slightly bent legs.

In order to estimate the effective damping ratio, an exponential function is fitted to the peak values of the recorded decay with amplitudes between 90% and 20% of the maximum peak value of the acceleration levels [30]. Figures 10-c and 10-d confirm that the applied excitation indeed leads to free vibration dominated by a single mode as assumed for the derivation of the effective damping ratio and natural frequency. Figures 10-e and 10-f present the natural logarithm and the least-squares approximation of peak amplitudes (y_i) with abscissa (x_i). The excellent fit that is obtained by the linear function with slope $-\delta$ (where δ represents the logarithmic decrement [31]), illustrates that the damping characteristics hardly depend on the vibration amplitudes.

Operational modal analysis

For the setups with ambient excitation, 9 or 21 persons were requested to stand still during 3 minutes, all adopting either an active or a passive posture. In addition, the persons were asked to walk at a slow, normal (self-selected) or fast speed along the main span of the bridge during 3 minutes (figure 9). The output-only data have been processed using the reference-based data-driven stochastic subspace identification (SSI-data/ref) algorithm [32, 33].

Characteristics of the coupled human-structure model

The dynamic behaviour of the footbridge is simulated with the experimentally identified natural frequencies and modal damping ratios and the mode shapes of the calibrated FE model of the empty structure. All individuals involved were weighted in the laboratory to determine their nominal mass. For each trial involving stationary persons, the location of every individual was determined. To account for inter-subject variability, the natural frequency f_{H1} and damping ratio ξ_{H1} of the human body models are sampled from the truncated Gaussian distributions defined for passive and active postures (in Eq. (7)). The mass ratios of the human body models are fixed to values of $\mu_{\text{H1}} = 0.95$ [-] and $\mu_{\text{H0}} = 0.05$ [-] for both postures. From the Monte Carlo simulations, the 5% and 95% percentile value of the effective natural frequency and damping ratio of the coupled crowd-structure model are retained.

Results

Figure 11 shows the effective natural frequency and modal damping ratio of the vertical bending mode for individuals in the passive posture, an active posture and walking at midspan.

For the passive posture (figures 11-a and 11-b), the frequency ratio is relatively high ($f_{\text{H1}}/f_{\text{B}} \approx [1.5, 2]$). As a result, the natural frequency of the footbridge decreases with the added (modal) mass. Despite the low mass ratio, the effective damping increases substantially which is owed to the very low inherent damping of the empty structure. Both effects are accurately predicted by the coupled model.

For figures 11-b and 11-e) that involve active postures, the frequency ratio is close to unity. As expected, this results in a small modification of the natural frequency and a very large value of the effective damping ratio, e.g. $\xi_{\text{eff}} > 3.5\% \ggg \xi_{\text{B}} = 0.2\%$ when 26 persons are involved. Although small variations of the natural frequencies of the human body models cause a large scatter in the predicted effective damping ratio, the trend is clear and corresponds well with the observations. The attained effective damping ratio is more than five times higher than for the passive posture.

Comparing the results in figures 11-e and 11-f with those in figures 11-c and 11-d, shows that the natural frequency and damping ratio obtained from the OMA involving walking persons, are in good agreement with the predictions which consider human body models with parameters corresponding to the active postures. This confirms that the presence of moving persons affects

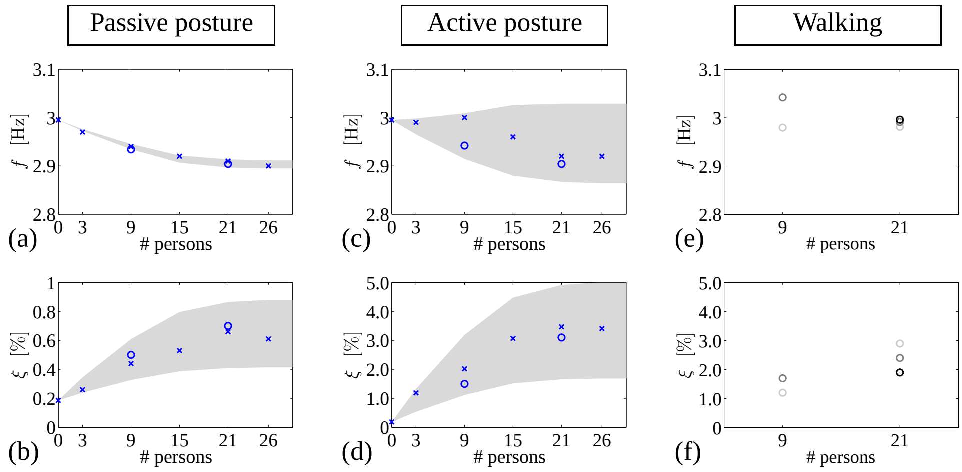

Figure 11: The effective natural frequency (a,c,e) and damping ratio (b,d,f) of the vertical bending mode: the 90% confidence region computed by the coupled human-structure model (grey area), identified from the free decay analysis (×) and identified from the OMA (○), for the human body in a (a,b) passive, or (c,d) active posture and for persons walking (e,f) at a low (light), normal (dark) and fast (black) speed.

the dynamic characteristics of the coupled system in a way which appears similar as in the case of stationary persons with two legs bent. The amount of added damping seems to decrease with the walking speed.

Figure 12 shows the effective natural frequency and modal damping ratio of the fundamental lateral-torsional mode, involving individuals in the passive posture, an active posture and walking. For both postures, the persons act as an additional mass, resulting in a small reduction in natural frequency. The latter can be explained by the fact that in both cases, the natural frequency of the persons is relatively high compared to the natural frequency of the considered mode ($f_{\mathrm{H1}}/f_{\mathrm{B}} > 1.5$).

However, figures 12-d and 12-e show that experimentally, an increase of the effective damping ratio is identified as well. It is believed that this mode, which is dominated by lateral motion, is also affected by HSI in the lateral direction. In order to verify this conjecture, the coupled model considered in addition a lateral SDOF system for each person with a fundamental natural frequency between 0.5 Hz and 1.0 Hz, i.e. in agreement with the preliminary results as reported by Matsumoto et al. [34]. Figures 12-d and 12-e show that the considered lateral HSI allows to explain the observed increase in effective damping.

Comparing the results in figures 12-e and 12-f with those in figures 12-c and 12-d, shows that the results from the OMA involving walking persons, are in good agreement with the predictions which consider both the vertical and horizontal body motion.

4.2 Charleroi footbridge

The second set of full-scale observations involves the Charleroi footbridge (see figure 13). The tests include ambient and pedestrian excitation. The latter consider 8 or 18 persons walking at a self-selected speed during 4 minutes. The output-only data have been processed using the reference-based data-driven stochastic subspace identification (SSI-data/ref) algorithm [32, 33]. The first three modes are the fundamental vertical bending mode ($\tilde{f}_1 = 1.66$ Hz, $\tilde{\xi}_1 = 0.13\%$, $m_1 = 122 \times 10^3$ kg), the second vertical bending mode ($\tilde{f}_2 = 5.16$ Hz, $\tilde{\xi}_2 = 0.29\%$, $m_2 = 122 \times 10^3$ kg) and the torsional mode ($\tilde{f}_3 = 5.56$ Hz, $\tilde{\xi}_3 = 0.48\%$, $m_3 = 88 \times 10^3$ kg),

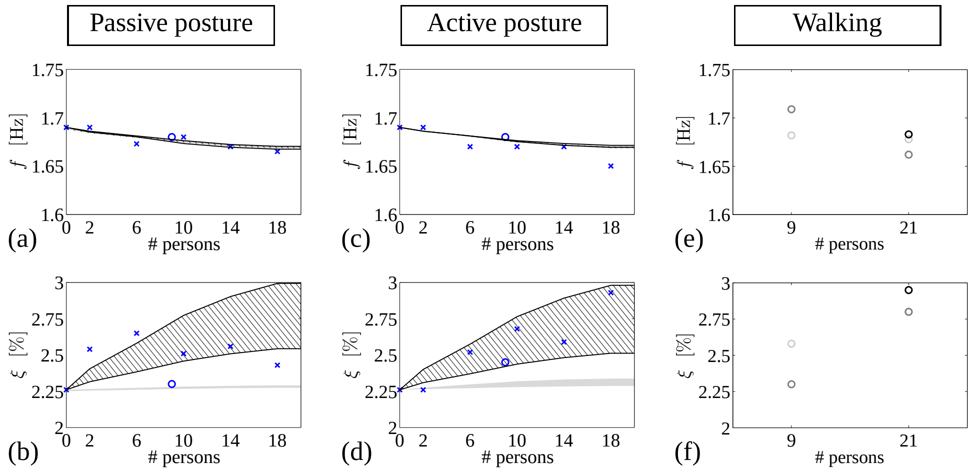

Figure 12: The effective natural frequency (a,c,e) and damping ratio (b,d,f) of the fundamental mode: the 90% confidence region computed by the coupled human-structure model (grey area), including in addition the horizontal human body models (hatched), identified from the free decay analysis (×) and identified from the OMA (○), for the human body in a (a,b) passive, or (c,d) active posture and for persons walking (e,f) at a low (light), normal (dark) and fast (black) speed.

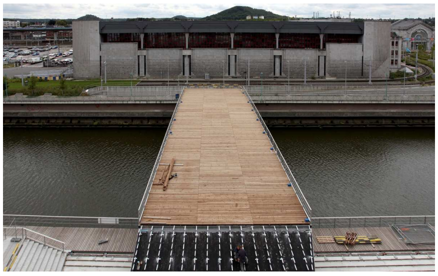

Figure 13: The Charleroi footbridge.

n_{H} [-]	$\tilde{f}_1$ [Hz]	$\tilde{\xi}_1$ [%]	$\tilde{f}_2$ [Hz]	$\tilde{\xi}_2$ [%]	$\tilde{f}_3$ [Hz]	$\tilde{\xi}_3$ [%]
-	1.66	0.13	5.16	0.29	5.56	0.48
8	1.65	0.16	5.15	0.46	5.54	0.56
18	1.65	0.19	5.15	0.83	5.53	0.93

Table 2: The identified natural frequencies and damping ratios of the first three modes of the Charleroi footbridge occupied with n_{ped} walking persons.

respectively. Due to the high modal masses and the high (≈ 2) and low (≈ 0.6) frequency ratios for the case of the first and the second and third mode, respectively, the effect of only 18 persons present on the bridge is expected to be limited. However, table 2 shows that as a result of the distinctly low inherent structural damping, even these low mass ratios lead to a non-negligible increase of the effective damping.

5 CONCLUSIONS

A parametric study is performed to investigate the interaction between the crowd and the low-frequency modes of the footbridge. The results show that taking into account HSI reduces the structural response. The most significant HSI-effect for vertical modes with a natural frequency up to 6 Hz, is in the effective damping ratio of the coupled system which is much higher than the inherent damping of the footbridge. The effective damping ratio increases monotonically with the mass ratio but is highly dependent on the natural frequency of the footbridge.

For practical design, the increase in effective damping can be considered relevant for modes with a natural frequency above 1.5 Hz. The most substantial increase is identified for modes with a natural frequency between 2.75 Hz and 5.0 Hz, as these are close to the natural frequency of active persons. In the case of (near-)resonant excitation at the second harmonic of the walking load (between 2.5 Hz and 5.0 Hz), the structural response reduces when HSI is taken into account, even for low mass ratios. For the case where (near-)resonant excitation is considered at the fundamental harmonic of the walking load (between 1.5 Hz and 2.5 Hz), the HSI-benefit is far less important and only relevant for high mass ratios or for structures with very low inherent damping ratios. For the considered range of footbridge parameters, the maximum attained effective damping is limited to 2%, 3.5%, 7% and 16% for pedestrian densities of 0.25, 0.5, 1.0 and 2.5 $\mathrm{persons/m^2}$, respectively.

The findings from the parametric study were verified by means of a comprehensive full-scale experimental study. It is shown that the coupled human-structure model is able to reproduce the experimentally identified modal characteristics of the coupled system. From these tests it is furthermore found that the interaction with the human body in the horizontal direction is of similar importance for structural modes with considerable lateral components.

6 ACKNOWLEDGEMENTS

This research is funded by the Agency for Innovation by Science and Technology in Flanders (IWT). Their financial support is gratefully acknowledged. The authors affiliated to KU Leuven are members of the KU Leuven - BOF PFV/10/002 OPTEC - Optimization in Engineering Center.

REFERENCES

[1] S. Živanović, A. Pavić, and P. Reynolds, "Vibration serviceability of footbridges under human-induced excitation: a literature review," *Journal of Sound and Vibration*, vol. 279, no. 1-2, pp. 1–74, 2005.

[2] C. Butz, M. Feldmann, C. Heinemeyer, and G. Sedlacek, "SYNPEX: Advanced load models for synchronous pedestrian excitation and optimised design guidelines for steel footbridges," Technical Report, Research Fund for Coal and Steel, 2008.

[3] V. Racić, A. Pavić, and P. Reynolds, "Experimental identification and analytical modelling of walking forces: a literature review," *Journal of Sound and Vibration*, vol. 326, pp. 1–49, 2009.

[4] R. Sachse, A. Pavić, and P. Reynolds, "Parametric study of modal properties of damped two-degree-of-freedom crowd-structure dynamic systems," *Journal of Sound and Vibration*, vol. 274, pp. 461–480, 2004.

[5] G. Busca, A. Cappellini, S. Manzoni, M. Tarabini, and M. Vanali, "Quantification of chances in modal parameters due to the presence of passive people on a slender structure," *Journal of Sound and Vibration*, vol. 333, pp. 5641–5652, 2014.

[6] M. Bocian, J. Macdonald, and J. Burn, "Biomechanically-Inspired Modelling of Pedestrian-Induced Vertical Self-Excited Forces," *Journal of Bridge Engineering*, vol. 18, pp. 1336–1346, 2013.

[7] L. Pedersen, "Implications of interaction between humans and structures," in *Proceedings of IMAC 33, the International Modal Analysis Conference*, 2015.

[8] C. Jones, P. Reynods, and A. Pavić, "Vibration serviceability of stadia structures subjected to dynamic crowd loads: a literature review," *Journal of Sound and Vibration*, vol. 330, pp. 1531–1566, 2011.

[9] J. Dougil, J. Wright, J. Parkhouse, and R. Harrison, “Human structure interaction during rhytmic bobbing,” *The Structural Engineer*, pp. 32–39, 2006.

[10] G. Subashi, Y. Matsumoto, and G. M.J., “Modelling resonances of the standing body exposed to vertical whole-body vibration: Effects of posture,” *Journal of Sound and Vibration*, vol. 317, pp. 400–418, 2008.

[11] Association Française de Génie Civil, Sétra/AFGC, *Sétra: Evaluation du comportement vibratoire des passerelles piétonnes sous l’action des piétons*, 2006.

[12] C. Heinemeyer, C. Butz, A. Keil, M. Schlaich, A. Goldack, S. Trometer, M. Lukic, B. Chabrolin, A. Lemaire, P. Martin, A. Cunha, and E. Caetano, “Design of lightweight Footbridges for Human Induced Vibrations - background document in support to the implementation, harmonization and further development of the eurocodes,” Technical Report, JRC-ECCS Scientific and Technical Reports - European Comission, 2009.

[13] GERB, “Tuned mass dampers,” reference list, GERB Engineering, March 2014.

[14] Maurer-Sohne, “Extract of reference list for tuned mass dampers,” reference list, Maurer-Sohne, February 2013.

[15] H. Bachmann, W. Ammann, and F. Deischl, *Vibration problems in structures: practical guidelines*. Springer, 1995.

[16] J. Brownjohn and A. Pavić, “Experimental methods for estimating modal mass in footbridges using human-induced dynamic excitation,” *Engineering Structures*, vol. 29, pp. 2833–2843, 2007.

[17] Research Fund for Coal and Steel, *Hivoss: Design of footbridges*, 2008.

[18] International organization for Standardization (ISO 10137), *Bases for design of structures - Serviceability of buildings and walkways against vibrations*, 2007.

[19] NBN EN 1991-2 NL, *Eurocode 1: Actions on structures - Part 2: Traffic loads on bridges*, 2013.

[20] NBN EN 1995-2, *Eurocode 5: Design of timber structures - Part 2: Bridges*, 2005.

[21] Y. Matsumoto and M. Griffin, “Dynamic response of the standing human body exposed to vertical vibration: influence of posture and vibration magnitude,” *Journal of Sound and Vibration*, vol. 212, no. 1, pp. 85–107, 1998.

[22] Y. Matsumoto and M. Griffin, “Mathematical models for the apparent masses of standing subjects exposed to vertical whole-body vibration,” *Journal of Sound and Vibration*, vol. 260, pp. 431–451, 2003.

[23] J. Brownjohn, P. Fok, M. Roche, and P. Omenzetter, “Long span steel pedestrian bridge at Singapore Changi Airport - part 2: Crowd loading tests and vibration mitigation measures,” *The Structural Engineer*, vol. 82, no. 16, pp. 28–34, 2004.

[24] J. Brownjohn, “Energy dissipation from vibration floor slabs due to human-structure interaction,” *Journal of Shock and Vibration*, vol. 8, pp. 315–323, 2001.

[25] K. Van Nimmen, K. Maes, S. Živanocić, G. Lombaert, G. De Roeck, and P. Van den Broeck, "Identification and modelling of vertical human-structure interaction," in *Proceedings of IMAC 33, the International Modal Analysis Conference*, 2015.

[26] International Organisation for Standardization, *ISO 5982:1981 Vibration and shock - Mechanical driving point impedance of the human body*, 1981.

[27] Y. Yang, J. Yau, and Y. Wu, *Vehicle-bridge interaction dynamics: With applications to high-speed railways*. World Scientific Publishing Co. Pte. Ltd., 2004.

[28] A. Doménech, P. Museros, and M. Martínez-Rodrigo, "Influence of the vehicle model on the prediction of the maximum bending response of simply supported bridges under high-speed railway traffic," *Engineering Structures*, vol. 72, pp. 123–139, 2014.

[29] K. Van Nimmen, G. Lombaert, I. Jonkers, G. De Roeck, and P. Van den Broeck, "Characterisation of walking loads by 3D inertial motion tracking," *Journal of Sound and Vibration*, vol. 333, pp. 5212–5226, 2014.

[30] F. Magalhães, A. Cunha, E. Caetano, and R. Brincker, "Damping estimation using free decays and ambient vibration tests," *Mechanical Systems and Signal Processing*, vol. 24, pp. 1274–1290, 2010.

[31] A. Chopra, *Dynamics of structures*. Prentice Hall, 1995.

[32] B. Peeters and G. De Roeck, "Reference-based stochastic subspace identification for output-only modal analysis," *Mechanical Systems and Signal Processing*, vol. 13, no. 6, pp. 855–878, 1999.

[33] E. Reynders, R. Pintelon, and G. De Roeck, "Uncertainty bounds on modal parameters obtained from Stochastic Subspace Identification," vol. 22, no. 4, pp. 948–969, 2008.

[34] Y. Matsumoto and G. M.J., "The horizontal apparent mass of the standing human body," *Journal of Sound and Vibration*, vol. 330, pp. 3284–3297, 2011.